EURATOM CEA

ASSOCIATION EURATOM C.E.A.

92260 Fontenay aux-Roses (France)

DEPARTEMENT DE PHYSIQUE DU PLASMA
ET DE LA FUSION CONTROLEE

DPh-PFC-SCP

EUR-CEA-FC-900

FR7706478

PRELIMINARY EXPERIMENTS ON ENERGY RECOVERY ON A NEUTRAL BEAM INJECTOR.

M. FUMELLI.

June 1977

Work executed under JET contract number B-FC-75

Table of Contents.

I. INTRODUCTION

Experimental tests of energy recovery are made on an injector of energetic neutral atoms in which the ion source (the circular periplasmatron) is operated at the ground potential and the neutralizer is biased at the high negative potential corresponding to the desired neutral beam energy (1). This mode of operation has the advantage that all the power supplies and control systems for the ion source do'nt have to be insulated for high voltage which implies also that the stored energy in stray capacitance is reduced (this energy is liberated when H.V. breakdown occurs and can damage the accelerating structure). In this disposition there is a strong electric field at the exit of the neutralizer which decelerates that fraction of the beam which is not converted into neutral atoms. This field offers the possibility of direct recovery of the energy of this fraction (by collecting it on an appropriate electrode biased near the ground potential). Although this latter point is relatively unimportant at present energies of 20 - 30 KeV, it becomes of major importance at the higher energies required for the next generation experiments (like the J.E.T.)

In an electrostatic energy recovery system it is necessary to prevent the acceleration of the neutralizer plasma electrons toward the collector of the decelerated ions (the recovery electrode).

A way to solve this problem is to create (by means of an appropriate electrode) a negative electric potential barrier for these electrons at the exit of the neutralizer. In initial experiments this potential barrier was created by means of a negatively biased plane grid placed across the beam (2) (3). A different method has been since developed which is more appropriate for high power beams. Instead of a plane grid a long cylindrical grid (called the suppressor grid) surrounding the beam is used (4). For a given negative potential (relative to the neutralizer) applied to this grid a plasma sheath develops at the periphery of the beam. At the entry of the grid the width of this sheat is generally much smaller than the beam radius. However, the ions are deflected by the electric field of the sheat outward through the grid. The ion density in the sheat is

thus decreasing as the beam propagates and the result is a sheat widening process which in turn causes more ions to be deflected. If the suppressor grid is sufficiently long the sheat will eventually fill the whole section of the beam, the potential on the axis will fall below the neutralizer potential and stop the electrons. Concurrently, most of the ions are deflected out of the suppressor. These ions can be decelerated and collected outside the region where the neutral beam propagates. A sheme of such a system is shown in fig. 1.

The cylindrical suppressor grid operation was studied in two different experimental arrangements. In addition different tests were made of the energy recovery effect ; the aim of these experiments of preliminary character was essentially to recognize the technical and physical problems involved in the subject, the actual experimental apparatus being not optimized for energy recovery.

The principal results of these differents measurements are reported and discussed in this paper.

2. EXPERIMENTAL

The first tests of the suppressor grid operation were made in an experimental situation in which a relatively high pressure existed in the suppressor grid region. The results (4) were encouraging and proved the feasibility of such a system, nevertheless relatively high suppressor grid potentials were needed to reflect the neutralizer plasma electrons owing the perturbing effect of neutral gas ionisation in the interior of the grid. To reduce this effect the injection line was modified : the neutralizer was lengthened and the suppressor grid was mounted in the interior of a large diameter tube placed inside the large vacuum chamber. This modification led to a substantial improvement of the pressure in the system.

A schematic view of the modified injection line is given in fig.2. The ion source is the circular periplasmatron described in (3). The ion beam is formed with a multi-aperture three electrode system. The electrodes are 0,3 cm thick copper disks with a 14,5 cm diameter free surface containing 450 holes of diameter 0,55 cm. The transparency is 0,65. The electrode spacings are 0,6 cm for the accelerating gap and 0,3 cm for the decelerating gap.

The neutralizer is a stainless steel tube of 15 cm interior diameter 70 cm in length.

When the injector was modified the neutralizer was lengthened by adding to it a tube of 23 cm in diameter and 55 cm in length in order to connect the injector to the suppressor grid system which is in the interior of the vacuum chamber.

The suppressor grid consists of a high transparency (88 %) cylindrical grid made of parallel stainless steel wires of Ø 1,5 mm. The diameter of the grid is 16 cm and its length 70 cm. This grid is mounted inside a tube, called the suppressor tube, 70 cm in length and 47 cm in diameter.

An annular plane grid, called the screen grid, of 67 % transparency, is mounted at the end of the suppressor tube. The fast ions pass through this grid ; they are decelerated and collected on the recovery electrode diameter 50 cm (see fig 2) placed at 14 cm from the screen grid. For some energy recovery test, as will see, the screen grid was removed from the system.

The energy and the profile of the neutral beam are measured in the test vacuum chamber with four concentric calorimeters of 5 - 10 - 15 - 20 cm respectively. These calorimeters are electrically insulated and are also used to measure the charged particles currents (electron for instance) coming from the injector. These calorimeters can be swept out of the beam. At the far end of the vacuum chamber, at about 3 m from the ion source, is mounted a large calorimeter of 30 cm diameter which also can be used to detect electrical signals.

The neutral beam components (resulting from the different ion species) can be analysed with a magnetic or electrostatic analyzer placed on the axis of the beam beyond the Ø 30 cm calorimeter.

The vacuum chamber is pumped at a speed of about 10^5 l/s, during the pulse the estimated neutral gas pressure inside the suppressor tube is about 10^{-4} Torr.

The principal electrical connections of the system are shown on fig. 2. THe neutraliser tube and the third of multi-aperture system electrode are at the same potential. They are connected, by means of a variable resistor R_n with the second multi-hole electrode which is connected to the H.V. generator, its potential being -V. When the beam is on, a positive current In (due to the slow ions resulting from charge-exchange collisions of ion beam with the neutral gas) polarises the neutralizer and the third electrode at the "decel" potential

$V_{decel} \simeq R_n I_n \simeq \frac{1}{10} V$; this potential is controlled by varying R_n.

Both the suppressor tube and grid are negatively biased with respect to the neutralizer by means of a capacitor bank in series with the H.V. generator. In several experiments the capacitor bank was shunted ; in these conditions the appropriate grid bias can be obtained

by adjusting the value of the resistor R_n which connects the neutralizer with the H.V. generator (see fig 2.). In this case the "decel" potential of the extraction system was created with an independent generator.

In the experiments made without the screen grid, the ion trajectories of the unneutralized beam were deflected and directed toward the recovery electrode by applying to the suppressor tube a positive potential (of the order of the neutralizer potential) with respect to the suppressor grid.

3. SUPPRESSOR GRID OPERATION

The critical voltage V^* of the suppressor grid is defined as the minimum value of the negative potential which must be applied to the suppressor grid with respect to the neutralizer to create an alectric potential barrier for the neutralizer plasma electrons. The critical voltage is determined experimentally as follows : a negative voltage is applied to the suppressor grid by the capacitor bank charged at a potential $V_s > V^*$. During the pulse the applied suppressor grid potential decreases by the suppressor current I_s which discharges the capacitor bank. When the value of the critical voltage is reached an increase of the neutralizer current I_n and of the H.V. generator drain current is observed corresponding to the loss of electrons. This electron current is also directly detected by measuring the electrical signals on the recovery electrode and on the calorimeters. An exemple of these measurements is shown on fig. 3.

It has been experimentally observed that the critical voltage increases with the beam intensity and that for the same ion beam current it has a maximum value for the energy which corresponds to the best beam focussing, that is to say at the perveance corresponding to the best beam transmission. This effect is shown on fig. 4. It can be seen that the critical voltage has a maximum for a beam perveance value :
$P \simeq 2{,}5.10^{-6}\ A/V^{3/2}$ which in previous beam transport measurements was found

to correspond to the best optics. In fig.5. are reported the measured values of V^* as a function of the extracted ion beam current. This current was increased up to 35 A, unfortunately it was impossible, for technical reasons, to increase the beam energy above 30 KeV. For this reason in these measurements the beam perveance was almost constant and near the optimum value at lower currents : $I_{ext} < 20$ A, but at higher currents the beam perveance increased and the beam optics deteriorates. This explains the saturation of V^* observed in the experimental points.

When the suppressor grid potential is inferior to the critical voltage $V_s < V^*$, an electron beam is accelerated toward the ground. Generally in these conditions strong electric oscillations are generated in the system. The accelerated electron current measurements for differents values of the ratio V_s / V^* are reported in fig. 6.

4. SUPPRESSOR AND NEUTRALIZER CURRENT MEASUREMENTS

The neutralizer current I_n and the suppressor I_s are not affected by the beam focussing. For suppressor voltages $V_s < V^*$, I_n increases by an amount corresponding to the current of accelerated electrons.

For $V_s \gg V^*$ both these currents are proportional to the extracted ion beam and they show a linear dependance with the neutral gas pressure. For a fixed beam current, I_n decreases and I_s increases with the gas pressure, the sum of these two currents giving the H.V. drain current which is very slightly affected by the pressure (these measurements were made by changing the gas pressure in the ion source).

In fig 7. are reported the measured values of I_s as a function of the pressure when the energy of the unneutralized beam is not recovered. In this figure the results obtained in the actual system are compared with previous measurements made in the former experimental disposition (see ref.(4).) in which the suppressor grid was inside a tube of smaller diameter, Ø 23 cm, which restricted the gas conductance. In the normal operating conditions in the first system we obtained $I_s \simeq I_{drain}$ and in the actual system $I_s \simeq 0{,}7\ I_{drain}$.

In the actual measurements there exists an additional current on I_s which is not completely explained. To this current contributes to some extent the secondary electron emission by fast ions bombardment of the suppressor tube and grid corresponding to the unneutralized beam fraction which cross the screen grid, is decelerated and, being not recovered, comes back to the system (this effect will be discussed later) This current was absent in the former experimental disposition due to the fact that the unneutralized beam could not escape from the suppressor tube.

5. ENERGY RECOVERY TESTS.

When a negative potential is applied to the recovery electrode a fraction of the unneutralized beam is collected by this electrode. In this case the H.V. drain current decreases proportionally to the collected ion current. The recovered electrical power is given by the product of this current decrement by the voltage drop between the suppressor system and the recovery plate.

This effect was tested in a first series of experiments in which generally Hydrogen gas was used. The H.V. drain current and the suppressor current I_s where monitored and during the pulse a negative time variable tension was applied to the recovery electrode. The variation of these currents was measured as a function of the recovery electrode potential and of the beam intensity. An exemple of these measurements is shown in the oscillograms of fig. 8.

The recovered drain current for a 20 A, 30 KeV beam (hydrogen gas) is given in fig. 9. as a function of the recovery electrode potential. This current saturates above a potential of about 4.5 KV. This value corresponds with the expected one by taking into account the inclination of the ions trajectories with respect to the recovery electrode.

The recovered drain current for two values of the extracted ion current is given in fig. 10. In these experiments the ion beam was accelerated at constant perveance and its intensity was varied by changing

the electrical power applied to the discharge of the ion source. The results of these measurements are in agreement with the expected values by taking into account the molecular and atomic content of the ion beam (only the full energy protons corresponding to the accelerated atomic ions can be recovered in the actual conditions), the inclination of the unneutralized beam trajectories, the screen grid transparency and the secondary electron emission effects by ion bombardment of this grid. However, some of these quantities are known with uncertainty.

For this reason a second series of energy recovery tests was made in a different and more simple experimental situation. The suppressor system was modified by removing the screen grid and instead of Hydrogen, Helium gas was used (only atomic species are present in the beam in this case). In these experiments it was necessary to apply to the suppressor tube a positive potential (relative to the suppressor grid) in order to deflect the trajectories of the unneutralized beam and allow them to reach the recovery electrode. In absence of this electric field, some of these trajectories are intercepted by the tube walls where they produce secondary electrons. Also secondary electrons are emitted by the fraction of the beam which is not recovered and comes back to the suppressor system (for instance when the recovery electrode is not adequately biased). Electrons can also be produced by ionisation of the residual gas in the suppressor system resulting from an inadequate pumping or the outgassing of the electrodes. All these electrons are accelerated toward the recovery electrode or the calorimeter plate where they can be detected electrically. In order to include this electron loss in the balance of the system, the ratio I_{ext}/I_{drain} of the extracted ion current over the H.V. generator current was measured under different conditions. The extracted ion beam current is deduced from the relation :

(I) $I_{ext} \simeq I_{drain} + I_r + I_c$

where I_r and I_c are respectively the recovery electrode and calorimeter measured currents (these measurements are not affected by the secondary electron emission because of the direction of the electric field on these electrodes). If $I_{ext} / I_{drain} < 1$ the balance of the system is negative. The maximum value of this ratio for an ideal system (without losses) is given by :

$$(2)\quad \left(\frac{I_{ext}}{I_{drain}}\right)_{max} = \frac{1}{F_o}$$

where F_o is the fraction of I_{ext} which is converted into neutrals. This limiting value has been reached in the actual system only by working at a relatively low beam power. For instance the measurements made on a 6 A extracted ion beam (H_e^+) 20 KeV energy are reported in fig. 11 and 12 ; at this energy the neutralisation efficiency (derived from published cross section data) is $F_o = 0{,}93$ the maximum value for I_{ext} / I_{drain} is then 1,075 which is in very good agreement with the measured values. In this case the fraction α of the unneutralized beam which is recovered is : $\alpha = 1$. A more general expression for the ratio I_{ext} / I_{drain} is :

$$(3)\quad \frac{I_{ext}}{I_{drain}} = \frac{1}{1 - (1-F_o)\left[\alpha(1+\gamma)-\gamma\right] + P_i}$$

where γ is the secondary electron emission coefficient and $P_i\ I_{ext}$ represent the electron current produced by ionisation of the residual gas. In these experiments the ionisation can be neglected ; from the measurements at $\alpha = o$ (when the recovery electrode is at zero potential see fig. 11) and from eq. 3. We deduce for γ the value $\gamma = 2$. In thi system I_{ext}/I_{drain} will be superior to one if $\alpha > 0{,}67$

In conclusion these preliminary tests show essentially the problems to be solved for an efficient recovery of the energy of the unneutralized beam fraction. A system optimised from the point of view of gas pumping, secondary electron emission and ion trajectories has been now designed (see fig.13) and will be operational at the end of this year. This system will be operated with and without a screen grid. In the latter case the deflection of the ion trajectories can be realised by means of a conical highly transparent grid shown in fig. 13.

APPENDIX I.

ENERGY BALANCE INCLUDING THE SECONDARY ELECTRON EMISSION EFFECTS

The secondary electron emission by fast ions bombardement reduces the efficiency of an electrostatic energy recovery system. For instance, if I is the part of the unneutralized beam current entering into the decelerating region of an energy recovery system, α being the recovery efficiency, the unrecovered current will come back to the negative electrodes of the suppressor system producing $I\ (1-\alpha)\gamma$ (γ is the secondary electron emission coefficient) electrons which are accelerated and which increase the H.V. generator drain current.

There will be no benefit of using such a system unless :

(4) $\alpha > \frac{\gamma}{1+\gamma}$

We can compare an injector having an energy recovery system with an injector which does not posses such a system and for which the electrical power spent to accelerate the beam is supposed to be $W = I_{ext}V$ (V is the potential corresponding to the beam energy). The fractional gain Ψ of electrical energy (the recovered energy is normalised to W) would be :

(5) $\Psi = \left[\alpha\ (1+\gamma\ )-\gamma\right] \frac{(V - \alpha V_{rec})}{V} R_o - P_s$

here $R_o = \frac{I}{I_{ext}}$; V_{rec} is the value (in eV units) of the residual energy of the recovered ions and P_s is the additional (normali ed to W) power spent to create the negative potential barrier at the exit of the neutralizer.

If the recovery system posses a screen grid, this grid avoid the acceleration of the secondary electrons emitted by the ions which return to the suppressor system and which are not intercepted by this grid. In these conditions if I is the unneutralised beam intensity at the exit of the grid and before the deceleration (this current produces $\frac{I\gamma}{I-T}$ secondary electrons) the H.V. generator drain current will be :

$$(6)\quad I_{drain} = I_{ext} - I\left[\alpha\,(1+\gamma^{*}) - \gamma^{*}\left(\frac{2-\gamma^{*}/\gamma}{1-\gamma^{*}/\gamma}\right)\right]$$

$\gamma^{*} = \gamma\,(1-T)$ where T is the screen grid transparency.
The screen grid system will be preferable if $T > \alpha$. The gain for a highly transparent grid will be approximately :

$$(7)\quad \Psi \simeq \left[\alpha\left(1+\gamma^{*}\right) - 2\,\gamma^{*}\right]\left(\frac{V-\alpha V_{rec}}{V}\right) R_o - P_s$$

The total electrical power spent to produce the neutral beam is
$P_{el} = (1-\psi)\, I_{ext}\, V$.

As an example if $R_o = 0,8$ (corresponding to an energy of 100 KeV for protons) and by assuming :

$\alpha = 0,9$; $\gamma^{*} = 0,15$; $P_s = 0,1$; $\frac{V_{rec}}{V} = 0,2$

from (7) we obtain $\Psi = 38\ \%$

APPENDIX II

Critical Voltage Evaluation

A simplified model which can be used for estimating purposes illustrates the sheat widening process in the beam plasma under the effect of the suppressor grid bias.

We know that between a plasma and a negative electrode (at the potential V^*) a positive space charge sheat develops whose thickness in the steady state can be evaluated (in the unidimensional case) from the Child Langmuir law :

$$(8)\quad X^2 = K\frac{V^{*\,3/2}}{J} \qquad \text{with } K = 5{,}45.10^{-8}\sqrt{\frac{Z}{M}}$$

where J is the plasma ion flux.

This stationary solution implies that the ion flux is maintained by some mechanism like the ionisation processes.

If the plasma ions are at rest and no ionisation occurs an ion flux across the sheat can be created by an increment in the time of the sheat thickness, that is :

$$(9)\quad J = \rho o\,\frac{dx}{dt}$$

where ρo is the unperturbed density and $\frac{dx}{dt}$ the speed of the moving sheat edge.

The identity of eq. (9) can be used in the eq. (8) if the variation of the flux in a caracteristic time τ of the system is small, that is if :

$$(10)\quad x > 2\,\frac{dx}{dt}\,\tau$$

where τ is the transit time of ions across the sheat given (in presence of space charge) by :

$$(11)\quad \tau = \frac{3x}{\sqrt{\frac{2eV^*}{m}}}$$

substituting in eq (8) the expression for J given by eq. (9) we obtain after integration the time t_o for the sheat thickness to be equal to D :

$$(12)\quad t_o = \frac{(D^3 - x_o^3)}{3} \quad \frac{\rho o}{KV^{*\,3/2}}$$

where x_o is the sheat thickness for t = 0

This model can be applied in the case of a parallel ion beam and in which x is a direction perpendicular to the ion trajectories (it describes the situation in a frame moving with the speed of the particles).

The distance L covered by the beam particules during the time t_o gives the length of the suppressor electrode

$$(13)\quad L = t_o \sqrt{\frac{2\,eV}{m}}$$

If we can neglect x_o in the expression for t_o we obtain :

$$(14)\quad L \simeq \frac{D^3\, J_o}{3\, KV^{*\,3/2}}$$

In the cylindrical case the formula for cylindrical-electrode space charge flow must be used instead of (8), nevertheless for estimating purpose the unidimensional treatment can be used the maximum discrepancy that can occur in the value of current density as calculated from the plane-electrode formula being nearly 20 per cent (see ref. 5).

J_o can be expressed :

$$(15)\quad J_o = \frac{P}{\pi R^2}\; V_o^{3/2}\; (1-F_o)$$

where P is the total perveance of the extracted ion beam. The formula (14) can be written in the cylindrical case

$$(16)\quad \frac{V^*}{V} = \left(\frac{1-F_o}{3\pi}\; \frac{P}{K}\; \frac{R}{L}\right)^{2/3}$$

(R is the suppressor grid radius)which gives the ratio of the suppressor voltage to the ion beam accelerating voltage.

In the actual experiments and in the situation of the optimum beam optics we have $\frac{P}{K} \simeq 46$, $(1-F_o) \simeq 0{,}2$, $\frac{R}{L} = 0{,}1$, by putting these values

in eq. (16) we obtain : $\frac{V^*}{V} \simeq 21\ \%$ which is in agreement with the experimental values. However this good agreement can be fortuitus due to the approximations which where used and the fact that in our particular experimental conditions the inequality expressed by eq. (10) is *not* well satisfied.

A more complete treatment of this problem has been done in ref (6).

Acknoledgements

We thank MM. Jacques GODAERT and Michel BLOCK for their technical assistance to this work.

REFERENCES

(1) M. Fumelli - Nuclear Inst. and Methods 118 (1974

(2) M. Fumelli, F.P.G. Valckx - Proc. of the 2nd Symp. on Ion Sources and Formation of IOn Beams - Berkeley, California (1974)

(3) M. Fumelli, F.P.C. Valckx - Nuclear Inst. and Methods 135 (1976)

(4) M. Fumelli, Ph. Raimbault - Proc. of the 9th Symposium on Fusion Technology, Pergamon Press Oxford O New York (1976)

(5) K.R. Spangenberg - Vacuum Tubes - Mc Graw-Hill Book Company (1948)

(6) Ph. Raimbault - EUR-CEA-FC-899

FIGURE CAPTION

Fig. 1. Scheme of the injection line and the suppressor grid energy recovery system.

Fig. 2. Schematic view of the cylindrical grid suppressor system and its principal electrical connexions. 1.Ion Source ; 2.Neutralizer ; 3.Suppressor grid ; 4.Recovery electrode ; 5.Tube grid.

Fig. 3. The effect of the plasma electron releases when the suppressor grid potential becomes inferior to the critical voltage V^*
a) Suppressor potential : 2 kV/div
b) Drain current : 5 A/div
c) Electron current on a plate placed in front of the beam : 1 A/div

Fig. 4. Variation of the critical voltage V^* with ion beam perveance

Fig. 5. Critical voltage V^* as a function of the extracted ion beam current.

Fig. 6. Ratio of the accelerated electron current to the extracted ion beam current I^e/I_{ext} as a function of the applied voltage to critical voltage ratio V_s/V^*.

Fig. 7. Dependence of the suppressor current I_s with the neutral gas pressure. Measurements without energy recovery.
a) Actual measurements in the modified experimental set-up
b) Previous measurements

Fig. 8. Energy recovery. Two pulses superposed, with and without recovery.
a) Drain current : 5 A/div.
b) Recovery electrode potential : 5 kV/div.
c) Neutralizer H.V. potential : 10 kV/div.
d) Suppressor system tube current : 3 A/div.

Fig. 9. Energy recovery. 20 A extracted ion beam. The recovered current as a function of the recovery electrode potential.

Fig.10. The recovered current for two values of ion beam current. Hydrogen beam. Ion beams perveance $P = 3.10^{-6}\ AV^{3/2}$

Fig.11. Energy recovery. Helium beam. Variation of $\frac{I_{ext}}{I_{drain}}$ with the recovery electrode potential

Fig.12. Energy recovery. Helium beam. Variation of $\frac{I_{ext}}{I_{drain}}$ with the deflection potential applied to the suppressor tube.

Fig.13 Schematic view of the energy recovery system prototype.

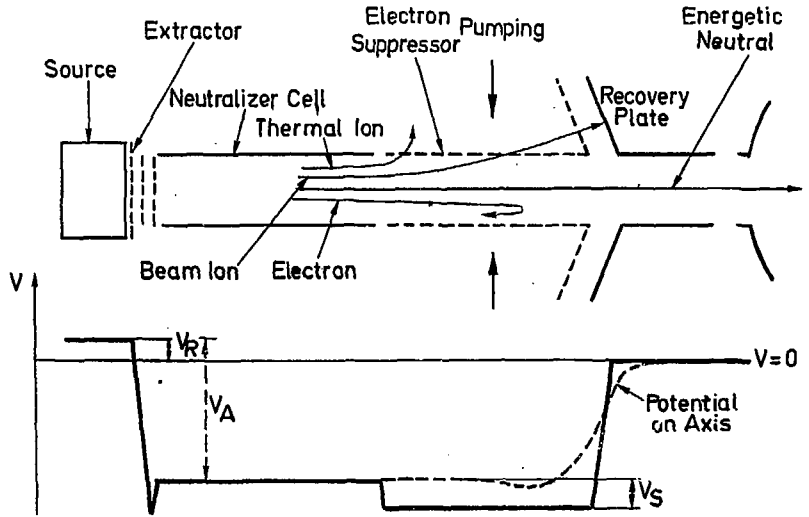
Source
Extractor
Neutralizer Cell
Thermal Ion
Electron Suppressor
Pumping
Recovery Plate
Energetic Neutral
Beam Ion
Electron
V
V_R
V_A
V=0
Potential on Axis
V_S

Fig. 1

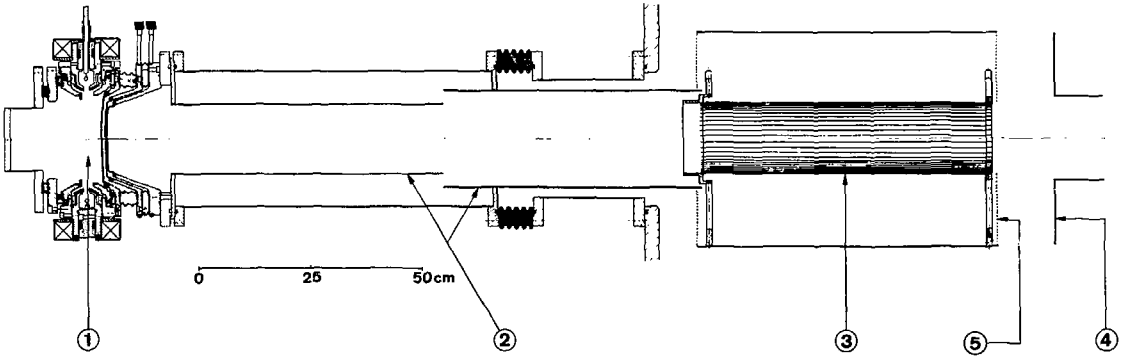

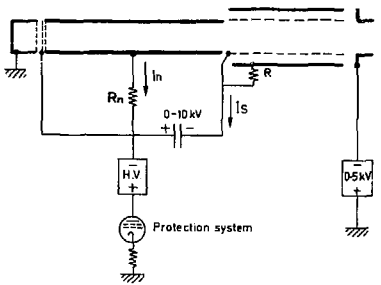

Fig. 2

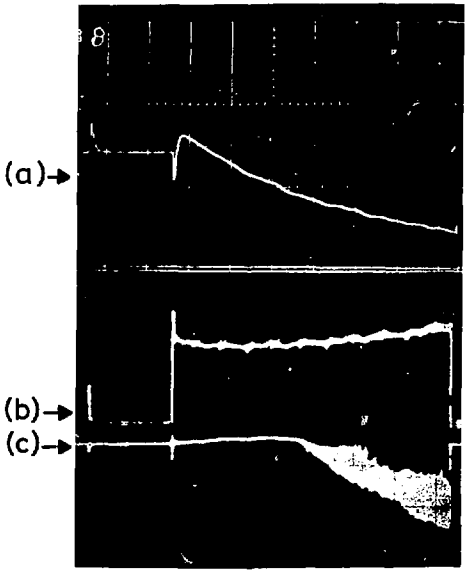

Fig. 3

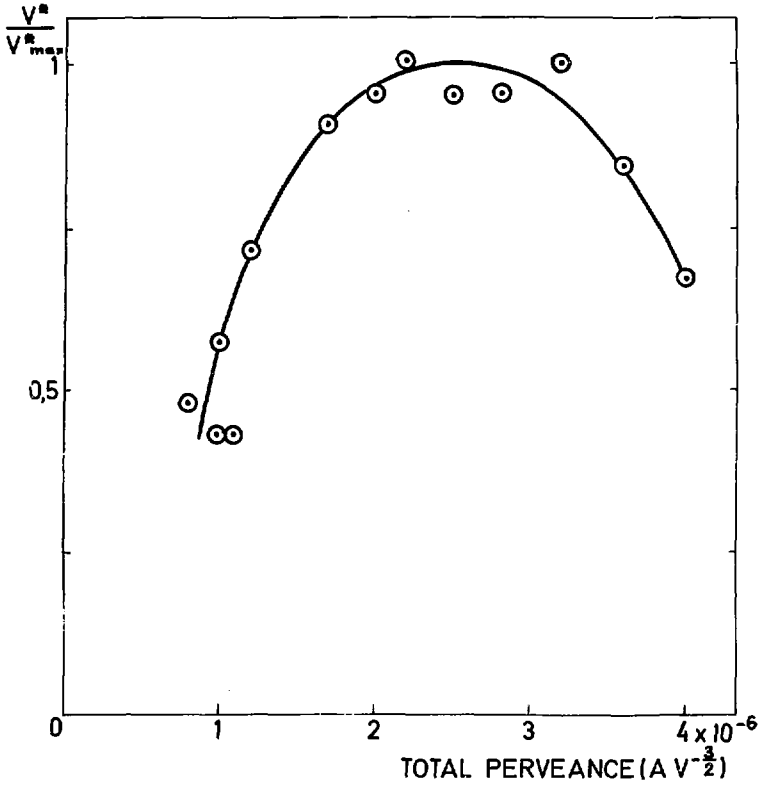

Fig. 4

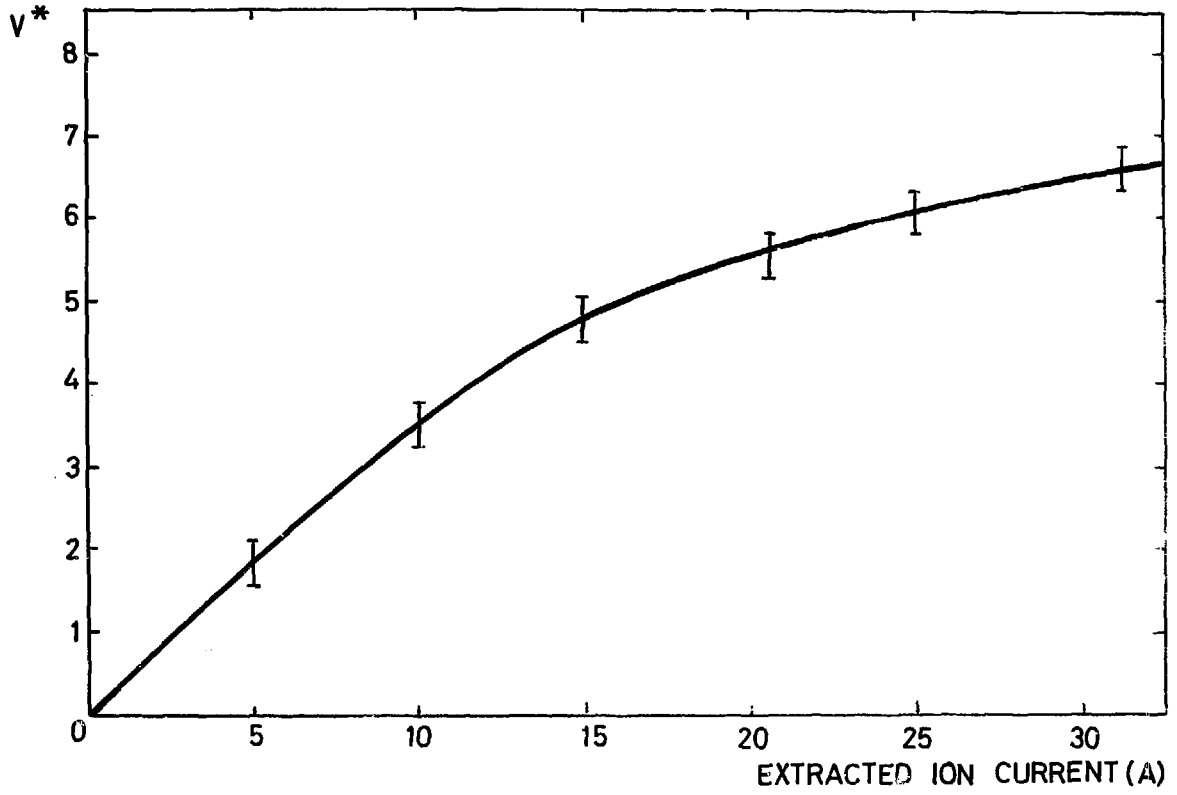

Fig. 5

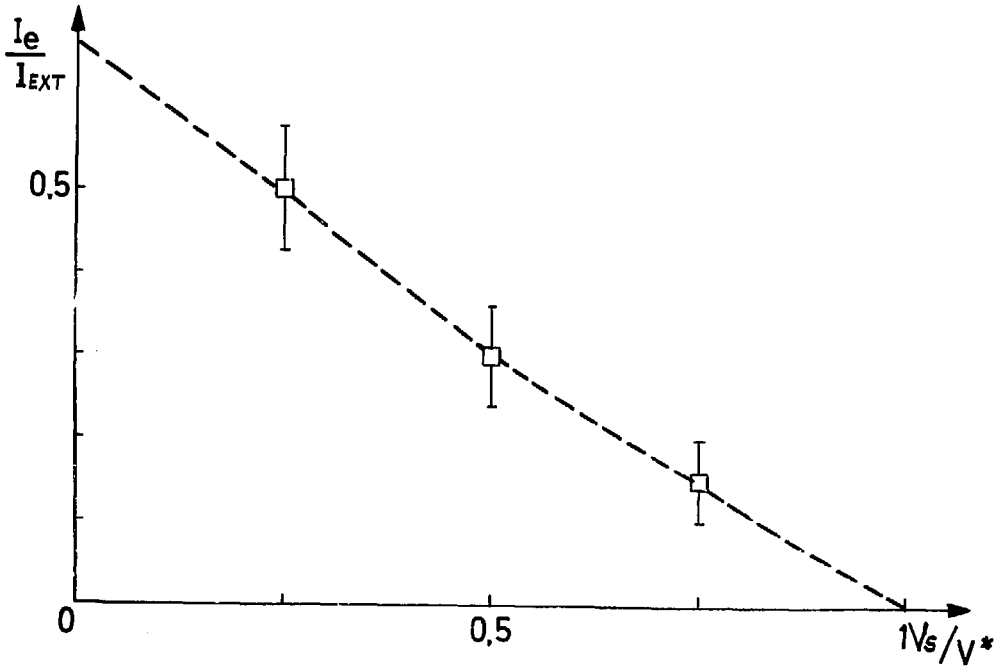

Fig. 6

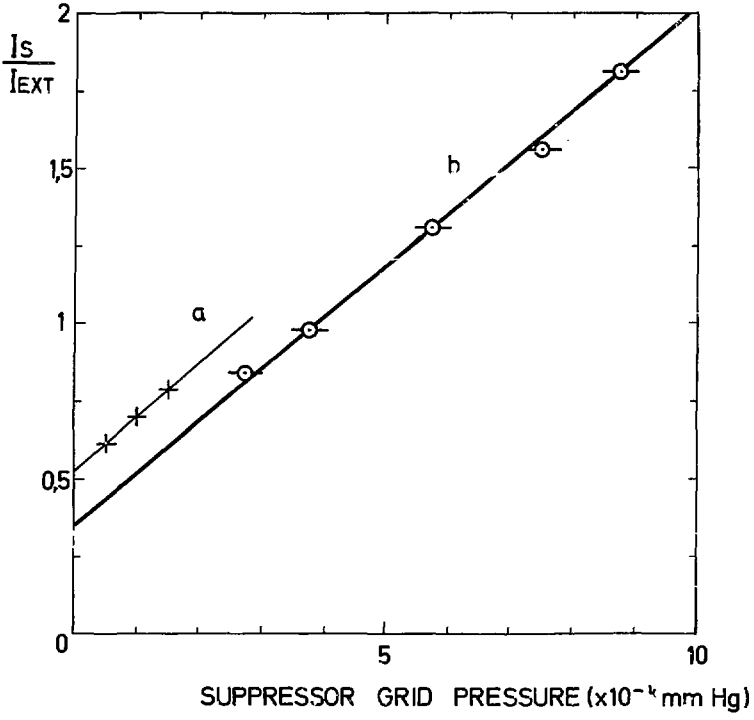

Fig. 7

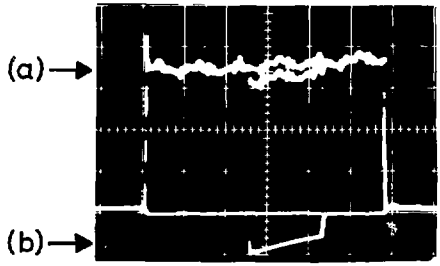

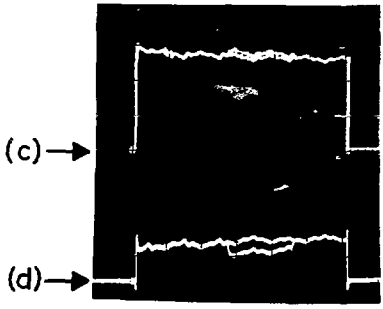

Fig. 8

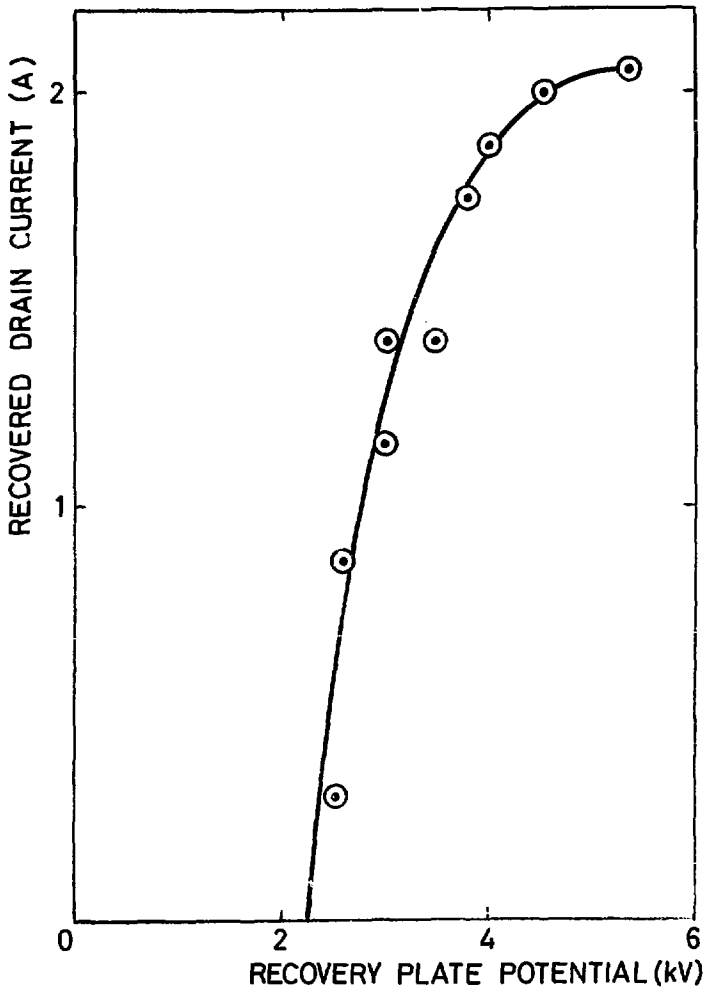
RECOVERED DRAIN CURRENT (A)
2
1
0
2
4
6
RECOVERY PLATE POTENTIAL (kV)

Fig. 9

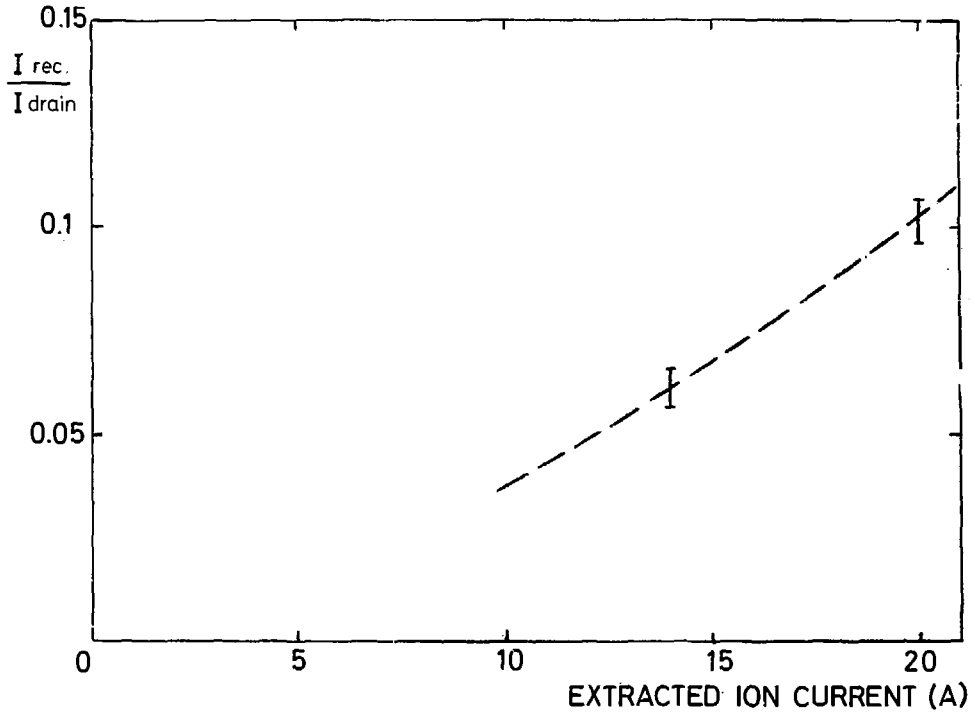

Fig. 10

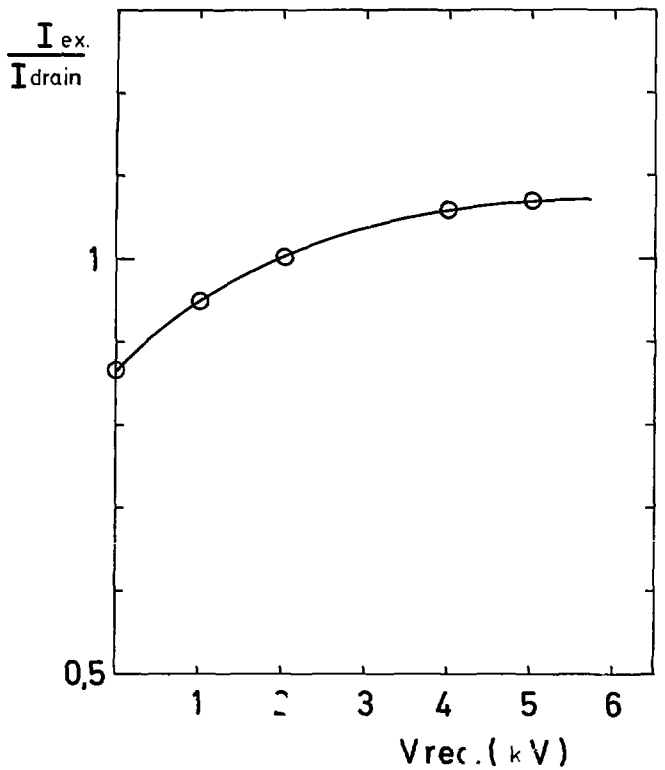

Fig.11

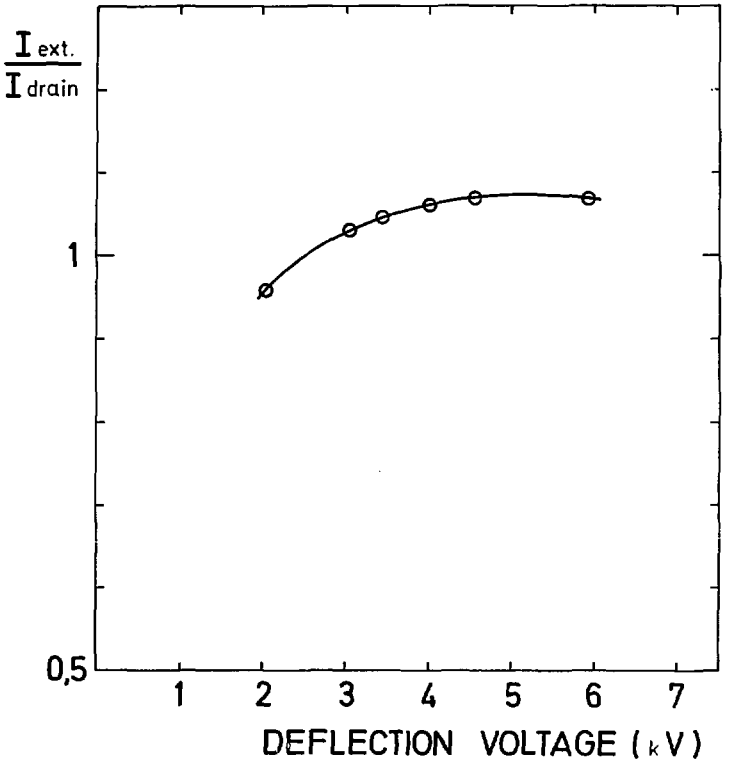

Fig. 12

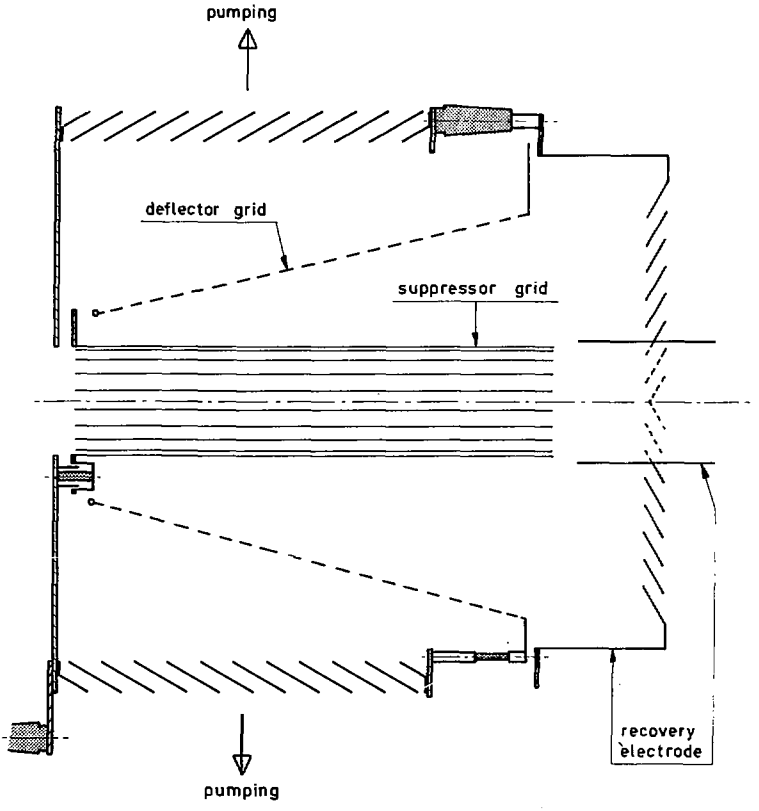
pumping
deflector grid
suppressor grid
recovery electrode
pumping

FIG. 13